THE JOURNAL OF PHYSICAL CHEMISTRY B

ARTICLE

pubs.acs.org/JPCB

Self-Assembly of Polydeoxyadenylic Acid Studied at the Single-Molecule Level

Sooyeon Kim, Jungkweon Choi,* and Tetsuro Majima*

The Institute of Scientific and Industrial (SANKEN), Osaka University, Mihogaoka 8-1, Ibaraki, Osaka 567-0047, Japan

Supporting Information

ABSTRACT: The investigation on the self-assembly of polydeoxyadenylic acid (poly(dA)) is highly important to fully understand its biological function and for its application in the field of nanotechnology. Using the fluorescence resonance energy transfer (FRET) technique, we report investigations for the self-assembly of adenine oligomers induced by pH and coralyne binding at the single-molecule level and in the bulk phase. Results presented here show that **A-motif 1** (Alexa488-5′-$(dA)_{20}$-3′-Cy5-5′-$(dA)_{20}$-3′-Alexa488) forms the wire-type duplex at acidic pH, whereas the same conformation of **A-motif 2** (Alexa488-5′-$(dA)_{20}$-3′-Cy5-3′-$(dA)_{20}$-5′-Alexa488) is induced by coralyne binding at neutral pH. These results indicate that poly(dA) at acidic pH forms a right-handed helical duplex with parallel-mannered chains, whereas the coralyne−poly(dA) binding induces a stable antiparallel duplex. Furthermore, we found that the antiparallel duplex of poly(dA) formed by coralyne binding has a rather extended and less twisted structure as compared to the parallel duplex of poly(dA) formed at acidic pH. On the other hand, from dilution experiments, we found that the parallel duplex formed at acidic pH is converted to "S-form", which has the single-stranded structure with short intramolecular double-stranded regions formed by intramolecular A:A base pairing, while the A-motif−coralyne assembly is dissociated into single strands below a certain concentration. The formation of S-form with a short intramolecular double-stranded region formed at acidic pH and very low concentration is confirmed by the quantitative analysis of FCS curve to measure the hydrodynamic radius of a molecule.

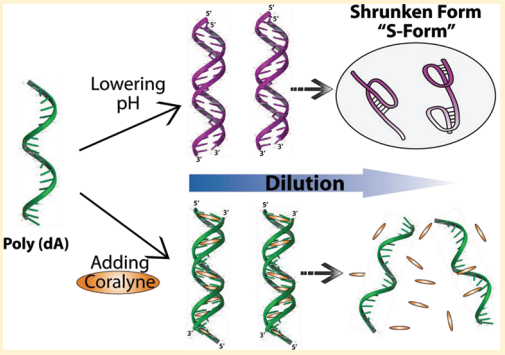

1. INTRODUCTION

In contrast to B-DNA that has a canonical right-handed double helical structure with Watson−Crick base pairing under the ordinary physiological conditions, repetitive DNA sequences under certain conditions may fold into non-B structure such as hairpin, triplex, cruciform, left-handed Z-form, tetraplex, etc.[1−3] Because these non-B structure-forming sequences induce the genetic instability and consequently may cause human diseases, the molecular mechanism for their genetic instability has been extensively investigated.[2] Furthermore, nanotechnology using non-B DNAs is an emerging field because non-B DNAs are robust and do not produce any toxic byproducts during a repetitive working cycle.[4−8] Among repetitive DNA sequences, single-stranded adenine-rich nucleic acids such as polydeoxyadenylic acid (poly(dA)) or polyadenylic acid (poly(A)) have attracted considerable attention because of their unique structure at acidic pH[9,10] and selective binding ability to small molecules.[11−15]

Because poly(A) is a tail component of mRNA in all eukaryotic cells and plays a key role in the stability of mRNA and translation initiation by its elongation and shortening,[16] the structure and the self-assembly of poly(A) have been intensively studied for several decades. Poly(A) is present as a right-handed helical single strand stabilized by the $\pi-\pi$ stacking of adenine bases at alkaline and neutral pH, whereas poly(A) at acidic pH forms a right-handed helical duplex with parallel-mannered chains and tilted protonated bases.[9] Rich et al. proposed that the parallel duplex is stabilized by two factors: the hydrogen bonds between two protonated adenine bases and electrostatic attraction between the positively charged protons at the N(1) atoms of the adenines and the negatively charged phosphate groups (Scheme 1a).[10] In addition, it was known that there are three different acidic conformations of poly(A): A-form, B-form, and frozen form.[17−21] On the other hand, small crescent-shaped alkaloids such as coralyne[11,13,22,23] and sanguinarine[14,24,25] can bind to poly(A) with a high affinity and induce a stable antiparallel duplex. The self-assembly of poly(A) formed by protonation or molecular binding is so-called "A-motif". Furthermore, A-motif is widely used for the nanotechnology because of its unique structure at acidic pH and selective binding ability to small molecules.[6,26−28]

Although poly(A) is of higher significance than poly(dA) in terms of biological relevance, poly(dA) may have more potential than poly(A) for further application in nanotechnology as a building block or sensory material because of the superior stability of DNA structure as compared to RNA structure. This being the case, an understanding on the self-assembly of poly(dA) is also

Received: September 15, 2011
Revised: November 9, 2011
Published: November 15, 2011

dx.doi.org/10.1021/jp208911t | J. Phys. Chem. B 2011, 115, 15399–15405

Scheme 1. (a) Illustration of Duplex Formation of Poly(dA) at Acidic pH (Left) and in the Presence of Coralyne Molecule (Right); and (b) Schematic Structures of A-motif 1 and 2

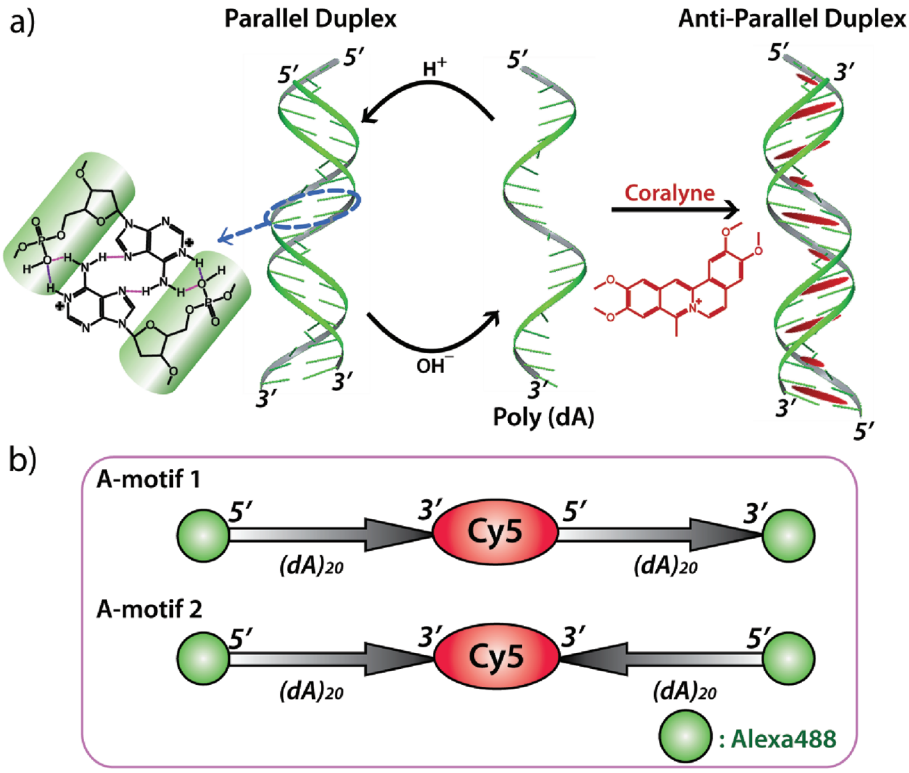

undoubtedly important. However, there have been very few studies that compare and characterize two distinct structures of poly(dA) duplex induced by pH and intercalator binding.

Here, using the fluorescence resonance energy transfer (FRET) technique, we investigated the self-assembly of adenine oligomer induced by pH and coralyne binding at the single-molecule level. For this study, we used two different oligonucleotides, **A-motif 1** (Alexa488-5′-$(dA)_{20}$-3′-Cy5-5′-$(dA)_{20}$-3′-Alexa488) and **A-motif 2** (Alexa488-5′-$(dA)_{20}$-3′-Cy5-3′-$(dA)_{20}$-5′-Alexa488). The strand polarities of the two oligonucleotides at the center are different as shown in Scheme 1b. Both end-sides were substituted by donor molecules (Alexa488), and the center of the oligonucleotide was substituted by acceptor molecule (Cy5). In addition, coralyne, one of the antileukemic drugs, is used as an intercalator to induce antiparallel duplex. Results presented here show that **A-motif 1** forms the wire-type duplex at acidic pH, whereas the same conformation of **A-motif 2** is induced by binding of coralyne at neutral pH. These results indicate that poly(dA) at acidic pH forms a right-handed helical duplex with parallel-mannered chains, whereas the coralyne−poly(dA) binding induces a stable antiparallel duplex. Furthermore, from dilution experiments, we found that the parallel duplex formed at acidic pH is converted to S-form, which has the single-stranded structure with short intramolecular double-stranded regions formed by intramolecular A:A base pairing, while the A-motif−coralyne assembly is dissociated into single strands under a certain concentration. Although the single-stranded structure with short intramolecular double-stranded region in poly(A) sequences has been proposed continuously, there was no report that experimentally evidenced the existence of intramolecular duplex in A-motif. For the first time, we successfully observed the existence of intramolecular double-stranded region in A-motif using various spectroscopic methods, including fluorescence correlation spectroscopy (FCS) and single-molecule spectroscopy. The result presented here suggests that there is a possibility of the existence of intramolecular duplex region in poly(A) tail in vivo, and this duplex region may affect the biological function of poly(A) tail.

2. EXPERIMENTALS METHODS

A-motif 1 (Alexa488-5′-$(dA)_{20}$-3′-Cy5-5′-$(dA)_{20}$-3′-Alexa488) and **A-motif 2** (Alexa488-5′-$(dA)_{20}$-3′-Cy5-3′-$(dA)_{20}$-5′-Alexa488) were obtained from Japan Bio Service. Structural details are demonstrated in Figure S1. The concentration of A-motif strand was determined by UV absorbance of Cy5 (ε_{650} = 250 000 M^{-1} cm^{-1}).[29] Coralyne chloride was purchased from Sigma-Aldrich and used without further purification. The concentration of coralyne was determined by UV absorbance of coralyne (ε_{420} = 14 500 M^{-1} cm^{-1}).[22] To prepare buffer solutions with a wide range of pH, 100 mM of Na_2HPO_4 and NaH_2PO_4 were used for pH 4.6−7.0, whereas H_3PO_4 and NaH_2PO_4 were used for pH 4.4−3.6 buffer solution. Fluorescence of Alexa488 and Cy5 is relatively pH-insensitive in the range of pH 3−8[30,31] (see also Figure S2).

The fluorescence and CD spectra were measured using a Horiba FluoroMax-4 and JASCO CD-J720, respectively. FCS experiments with various pH solutions were measured with a time-resolved fluorescence microscope using confocal optics (MicroTime 200; PicoQuant, Berlin-Adlershof, Germany).

In the single-molecule FRET experiment, 1 nM A-motif solutions containing 10% β-Mercaptoethanol by volume and

1 mM Trolox were prepared. Trolox and β-mercaptoethanol are used to reduce photoblinking and photobleaching (Figure S3).[32] To observe fluorescence intensity trajectories (FITs) of freely diffusing single molecules, 60 μL of each sample was loaded into the microchamber made by a 1 in. glass coverslip and Secure-Seal (S24733, Invitrogen). FITs were measured with the same confocal optics (MicroTime 200; PicoQuant, Berlin-Adlershof, Germany) and two single photon avalanche photodiodes (Micro Photon Devices, PDM 50CT and 100CT) for the simultaneous detection of the FRET donor and acceptor. All samples were excited through an oil objective (Olympus, UPlanSApo, 1.40 NA, 100×) with a 485 nm pulsed laser (Pico Quant, full width at half-maximum 120 ps) controlled by a PDL-800B driver (PicoQuant). The excitation power of about 65 μW was used. Bandpass filters (Olympus, BA510-550 and 690/70), and 75 μm pinhole were used for spatial filtering to reject out-of-focus signals. The data collected using the PicoHarp 300 TCSPC module (PicoQuant) were stored in the time-tagged time-resolved mode (TTTR), recording every detected photon with its individual timing, which were used for the single-molecule analysis. Each FIT was taken for 1 min with a binning time of 1 ms. All of the experimental data were obtained at room temperature.

3. RESULTS AND DISCUSSION

Figure 1 shows the fluorescence spectra of **A-motif 1** and **2** as a function of pH. As shown in Figure 1, the fluorescence intensities of Alexa488 attached to **A-motif 1** and **2** are decreased by lowering pH. Especially, the fluorescence quenching of **A-motif 1** is much more dramatic than that of **A-motif 2**. Because the fluorescence intensity of Alexa488 is independent in the range of pH 4.0−10.0, the changes in the fluorescence intensities of A-motif with decreasing pH are closely related to the conformational change of A-motif. Interestingly, as shown in Figure 1c, **A-motif 1** shows an abrupt transition of apparent FRET efficiency ($I_A/(I_A + I_D)$) at about pH 4.0, whereas that of **A-motif 2** shows a constant value (~0.1). This discrepancy is probably due to the different conformation of the pH-induced self-assembly of **A-motif 1** and **2**, resulting in the distinct FRET efficiencies. As mentioned above, poly(A) at acidic pH forms a right-handed helical duplex with parallel-mannered chains and tilted protonated bases. Considering the sequence of **A-motif 1** and **2**, which have different directions of phosphate backbone, **A-motif 1** at acidic pH can form the dimeric duplex or wire-type duplex, whereas **A-motif 2** can form the dimeric duplex or hairpin-type duplex (Figure S4). Among these structures, only wire-type duplex can induce a high FRET efficiency due to the fast energy transfer from the donor to the acceptor because of close proximity. In light of these results, we conclude that **A-motif 1** at acidic pH can dominantly form the wire-type duplex leading to a high FRET efficiency, whereas **A-motif 2** can form the dimeric duplex or hairpin-type duplex. Here, it is noteworthy that the apparent FRET efficiency of **A-motif 2** was not affected by DNA duplex formation even if the fluorescence intensities of the donor and acceptor of **A-motif 2** slightly decrease due to the $\pi-\pi$ interaction between two dyes by the formation of a dimeric or hairpin-type duplex. This means that the change of the apparent FRET efficiency shown in this study is mainly attributed to changes of interdye distances.

On the other hand, we also investigated the self-assembly of A-motif induced by coralyne binding at neutral pH (Figure 2). In

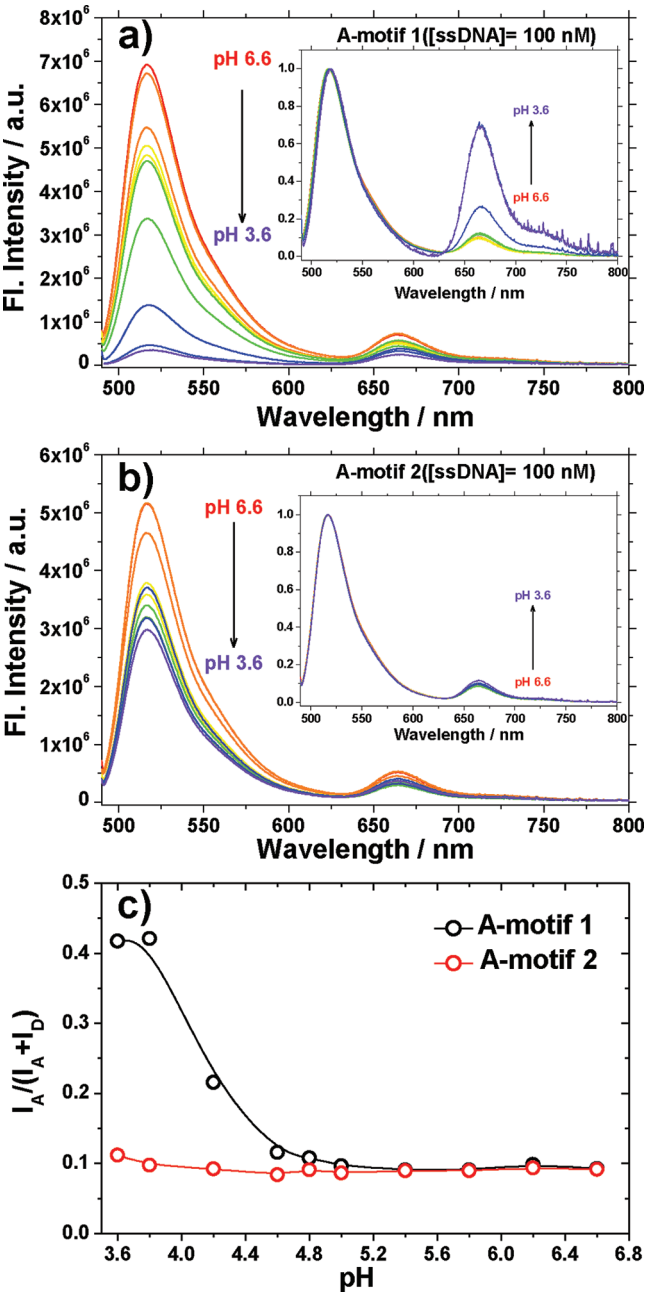

Figure 1. Fluorescence spectra of **A-motif 1** (a) and **A-motif 2** (b) in various pH solutions. The insets show the normalized fluorescence spectra at 518 nm. [ssDNA] = 100 nM, λ_{Ex} = 485 nm. (c) The ratio of the fluorescence intensities of acceptor to total emission ($I_A/(I_A + I_D)$) of **A-motif 1** (black) and **A-motif 2** (red) in various pH solutions.

contrast to the A-motif duplex induced by pH, the FRET efficiency of **A-motif 2** was increased considerably by adding coralyne, whereas that of **A-motif 1** was decreased. As explained earlier, coralyne induces antiparallel duplex of poly(A) or poly(dA) by the intercalation into four adenine bases.[11,33] Considering the sequence of each nucleotide (see Figure S4), **A-motif 2**−coralyne assembly at neutral pH has only a wire-type duplex resulting in a high FRET efficiency, whereas **A-motif 1** can form several structures such as a dimeric duplex or hairpin-type duplex (Figure S4). Therefore, the increase of the FRET efficiency observed for **A-motif 2** indicates that **A-motif 2**−coralyne

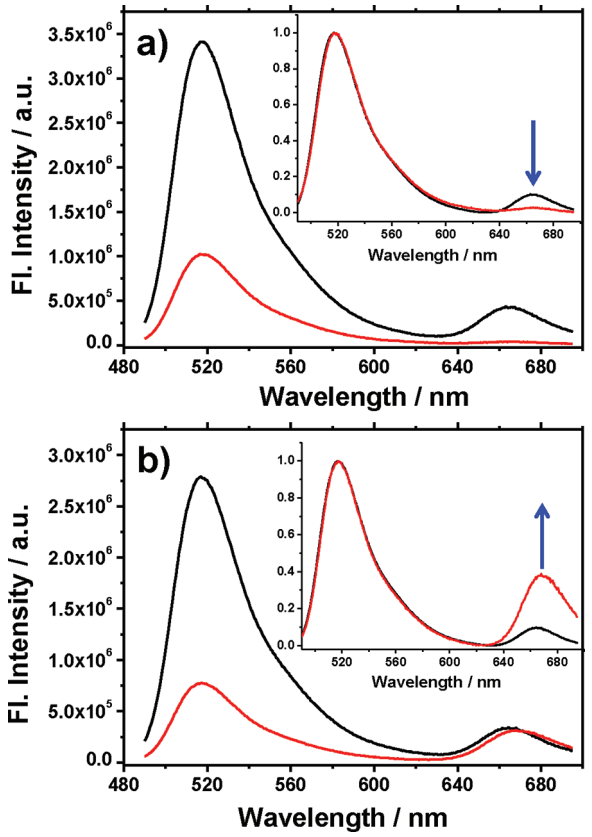

Figure 2. Fluorescence spectra of **A-motif 1** (a) and **A-motif 2** (b) in the absence (black) and presence (red) of coralyne. The insets show the normalized fluorescence spectra at 518 nm. [ssDNA] = 100 nM ([adenine] = 4 μM; [coralyne] = 1 μM; λ_{Ex} = 485 nm). The direction of arrows represents the change in normalized fluorescence emission of Cy5 upon adding coralyne.

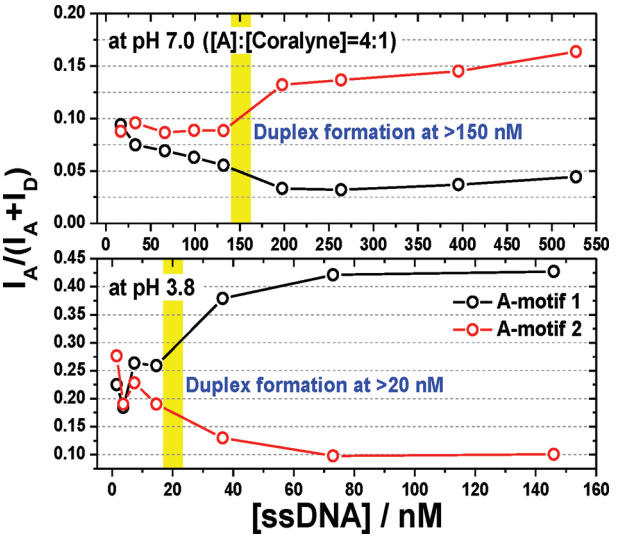

Figure 3. Changes in the ratio of the fluorescence intensities of acceptor to total emission ($I_A/(I_A + I_D)$) accompanied by the conformational change of self-assembly of A-motif at acidic pH (lower) and in the presence of coralyne (upper) by the dilution. ssDNA stands for a single strand of 40-mer A-motif DNA. The molar ratio of [ssDNA] to [coralyne] in all samples is adjusted to be 4:1. Approximate transition regions are depicted as a yellow box.

assembly at neutral pH has only a wire-type duplex structure. By contrast, **A-motif 1** forms a dimeric or hairpin-type duplex with coralyne. Additionally, using an atomic force microscopy (AFM), we could observe the wire-type structures of **A-motif 1** and **2** induced by the acidic condition and coralyne molecule, respectively, supporting that poly(dA) at acidic pH forms a right-handed helical duplex with parallel-mannered chains, whereas the binding of coralyne induces an antiparallel duplex (Figure S5).

Here, it is noteworthy that the parallel dimeric duplex formed at acidic pH does not affect the FRET efficiency (**A-motif 2** in Figure 1c), whereas the antiparallel dimeric duplex formed with coralyne leads to the decrease of the FRET efficiency from 0.1 to 0.03 (**A-motif 1** in Figure 2a). This result means that the intercalation of coralyne into the four adenine bases results in the elongation of the helical structure of poly(dA)-coralyne assembly (~1 nm). This result well agrees with the theoretical result of Joung et al. that the antiparallel duplex formed by coralyne binding has a rather extended and less twisted structure as compared to canonical B-DNA.[34]

Concentration of the poly(A) is an important factor in the self-assembly of poly(dA) or poly(A). According to the previous study on the dissociation of poly(A) duplex,[33] the poly(A)−coralyne assembly undergoes a sharp transition toward a single strand as a function of poly(A) and ligand concentration. In other words, the poly(A)−coralyne assembly begins to be dissociated into single strands under a certain critical concentration. Here, using the change in the FRET efficiency accompanied by the dilution, we further investigated the concentration effect on the self-assembly of poly(dA) induced by pH and coralyne binding. As shown in Figure 3, the FRET efficiency of **A-motif 2** (red), which forms a wire-type duplex in the presence of coralyne at neutral pH, is decreased from 0.17 to 0.1 as the sample is diluted from [ssDNA] = 527.4 to 16.5 nM, whereas that of **A-motif 1** (black) is increased from 0.03 to 0.1 (see Figure S6). In contrast to the result of A-motif−coralyne assembly, the FRET efficiency of **A-motif 1**, which forms a wire-type duplex at acidic pH, is decreased from 0.45 to 0.2 as the sample is diluted from [ssDNA] = 146.0 to 1.5 nM, whereas that of **A-motif 2** is increased from 0.1 to 0.2. These results indicate that the self-assembly of poly(dA) formed by pH and coralyne binding is dissociated by the dilution (see Figures S6 and S7). Furthermore, as depicted in Figure 3, the parallel duplex formed at acidic pH begins to be dissociated at about [ssDNA] = 20 nM, whereas the antiparallel A-motif duplex formed with coralyne at neutral pH begins to be dissociated at about [ssDNA] = 150 nM. These results mean that the parallel duplex of A-motif formed at acidic pH is more stable than another induced by coralyne intercalation. The different transition concentrations (or critical concentration) can be explained by the distinct duplex structure. In the case of A-motif−coralyne assembly, the two single-stranded poly(dA)s and coralyne molecules with the ratio of one coralyne to four adenine molecules are incorporated in the duplex formation, depending on the concentration of single-stranded poly(dA) as well as coralyne. However, because the parallel duplex at acidic pH without coralyne is formed by A:A base-pairing due to the hydrogen bonds between two protonated adenine bases, the parallel duplex formation depends on the concentration of only single-stranded poly(dA). Thus, the parallel duplex formed at acidic pH is relatively less affected by the concentration of DNA.

Interestingly, **A-motif 1** and **2** at very low concentration and acidic pH showed the FRET efficiencies of 0.2, while **A-motif 1**

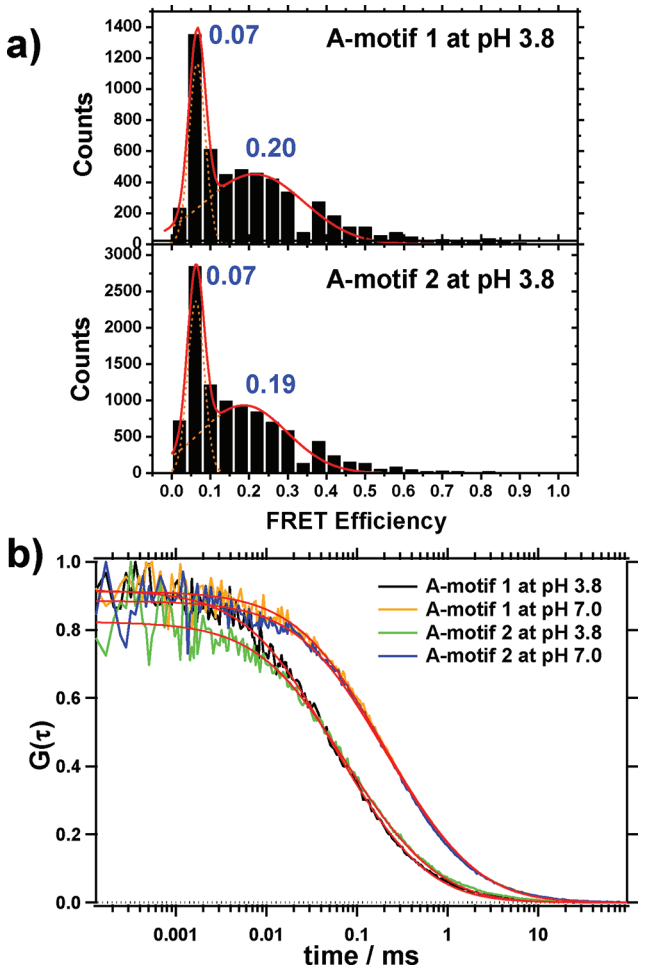

Figure 4. (a) Single-molecule FRET histograms of **A-motif 1** (upper) and **2** (lower) at pH 3.8. Both of them show a zero-efficiency peak and one low-FRET population (approximately, $E \approx 0.2$). (b) FCS curves and the fitting results (red) of A-motif at pH 3.8 (black, **A-motif 1**; green, **A-motif 2**) and 7.0 (yellow, **A-motif 1**; blue, **A-motif 2**) under an acidic condition.

and **2** in the presence of coralyne at very low concentration and neutral pH showed the FRET efficiencies of 0.1. The FRET efficiency of 0.1 observed in the presence of coralyne at very low concentration and neutral pH is close to those of single-stranded **A-motif 1** and **2** observed at neutral pH (Figure 1c). Thus, the observation of FRET efficiency of 0.1 in the presence of coralyne at very low concentration implies that the A-motif−coralyne assembly is dissociated into the single-stranded structure by the dilution. This result is consistent with that reported by Hud and co-workers.[33] However, the FRET efficiency of 0.2 observed at very low concentrations and acidic pH is 2 times higher than those of single-stranded **A-motif 1** and **2** observed at neutral pH, indicating that the parallel duplex formed at acidic pH and low concentration was converted to a more compact conformation rather than an extended single-stranded structure.

To confirm the existence of the alternative acidic conformation at extremely low concentration, single-molecule FRET experiment was carried out. Single-molecule fluorescence spectroscopy provides an insight into the behavior of each individual molecule and consequently allows a detailed observation of subpopulations in structures and dynamics hidden under ensemble-averaged results.[35−38] Figure 4a displays the FRET efficiency distributions determined from the FITs of single-molecule **A-motif 1** and **2** in the pH 3.8 solution. As depicted in Figure 4a, the FRET efficiency distributions of **A-motif 1** and **2** at pH 3.8 show two distinct peaks (0.07 and 0.20), whereas the FRET histogram observed at pH 7.0 shows a single FRET peak centered at almost zero (~0.03) (Figure S8). Considering the experimental error, $E_{FRET} \approx 0.03$ and 0.07 determined at pH 3.8 and 7.0 may be attributed to the same structural species. Because **A-motif 1** and **2** have a single-stranded structure at neural pH as shown in Figure 1c, the low FRET efficiency observed at pH 3.8 and 7.0 ($E_{FRET} \approx 0.07$) comes from the single-stranded structures of **A-motif 1** and **2**. On the other hand, the E_{FRET} of ~0.2 observed at pH 3.8 is close to those ($E_{FRET} \approx 0.20$) of **A-motif 1** and **2** determined from the dilution experiments, supporting that the parallel duplex formed at acidic pH was converted to the alternative acidic conformation rather than an extended single-stranded structure. The r_{D-A}'s for the structural species with $E_{FRET} \approx 0.2$ are calculated to be 6.6 nm. This value is shorter than that of single-stranded **A-motif 1** and **2** ($r_{D-A} \approx$ 7.4 nm), indicating that the structural species with $E_{FRET} \approx 0.2$ at low concentration has a more compact conformation as compared to the single-stranded structure. Here, we named the new species observed at extremely low concentration and acidic pH as "S-form" because this species exhibits a shrunken structure as compared to the extended single-stranded structure of poly(dA).

Here, we consider the individual conformations of the S-form of **A-motif 1** and **2** observed at extremely low concentration and acidic pH. Several studies on the pH dependent conformational transition of poly(A) proposed that there are three different acidic conformations of poly(A) depending on the extent of protonation of the molecule: A-form, B-form, and frozen form.[17−21] As pH is lowered from neutral pH, B-form appears at the pH just below the pK_a of N(1) atom of adenine and is stabilized by the partial protonation of adenine bases. When pH is further decreased, A-form is formed, which is tightly packed with fully protonated A:A bases. Another acidic form is a frozen form, which is observed only below about pH 4.0. The conformation of frozen form can be described as a grid-like aggregate consisting of alternating, variably sized, single-stranded regions linked with short double-stranded region. Thus, S-form, observed at pH 3.8 in this study, may be compared to frozen form, which has a disordered grid-like aggregated structure below pH 3.8. However, because frozen form exists only at high concentration and its formation is prevented by the dialysis, the S-form, which is observed only at extremely low concentration (<20 nM) in this study, is not a kind of assembly such as a duplex or aggregate. In other words, this means that the S-form observed in this study is not a frozen form, which is made of many poly(A) molecules. In light of these results, we propose that S-form observed at acidic pH and low concentration may have a short intramolecular double-stranded region. As the concentration of A-motif at acidic pH is lowered, the molar ratio of proton against A-motif is significantly increased. Therefore, the single-stranded DNA formed by dilution greatly interacts with proton, leading to the double-stranded regions formed by intramolecular A:A base pairing.

If the structure of A-motif at acidic pH and low concentration has a short intramolecular double-stranded region, its hydrodynamic radius should be shorter than that of the single-stranded structure. To further confirm the existence of intramolecular double-stranded regions in A-motif, we measured the change in

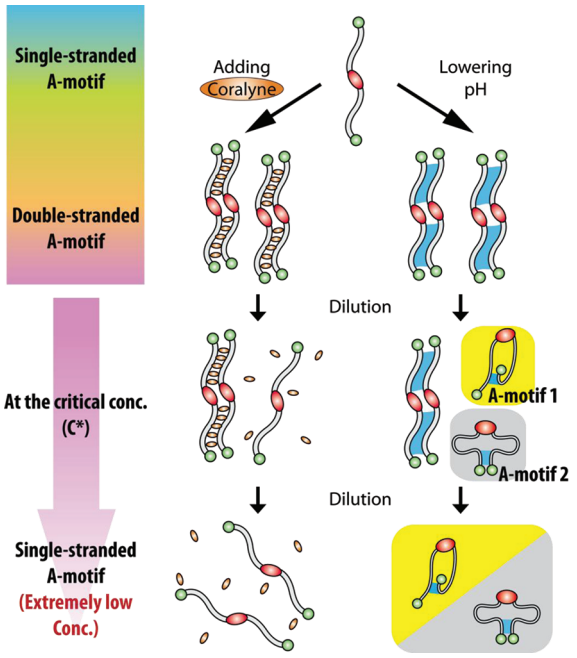

Figure 5. Representative formation and dissociation processes of A-motif induced by coralyne molecule (orange) and low pH. Sky blue region represents A:A base pairing region under an acidic condition. Two distinct conformations of **A-motif 1** and **2** at low concentration under an acidic condition are depicted in yellow and gray boxes, respectively. See Figures S9 and S10 for detailed dissociation pathways for **A-motif 1** and **2**, respectively.

the hydrodynamic radius of **A-motif 1** and **2** using FCS. FCS is a very valuable tool to observe the hydrodynamic radius from the translational diffusion of a biomolecule.[30,38,39] In FCS, autocorrelation function ($G(\tau)$) of the fluorescence intensity is given by

$$G(\tau) = \frac{\langle I(t)I(t+\tau)\rangle}{\langle I(t)\rangle^2} \quad (1)$$

where $I(t)$ is the fluorescence intensity at time t, $I(t+\tau)$ is the fluorescence intensity after a time lag τ, and $\langle\rangle$ denotes the time average over the total observation time. The autocorrelation function for diffusion in three dimensions can be expressed by

$$G(\tau) = \frac{1}{N}\left(1+\frac{\tau}{\tau_{\mathrm{diff}}}\right)^{-1}\left(1+\left(\frac{s}{u}\right)^2\frac{\tau}{\tau_{\mathrm{diff}}}\right)^{-1/2} \quad (2)$$

where N is the average number of molecules in the observed volume, τ_{diff} is the molecular diffusion time, s is the radius of the measurement area, and u is one-half of its axial length. Figure 4b shows FCS curves of **A-motif 1** and **2** recorded at pH 3.8 and 7.0. From the quantitative analysis of FCS curves with eq 2, diffusion times (τ_{diff}) of **A-motif 1** and **2** at pH 7.0 are determined to be 2.28 ± 0.18 and 2.35 ± 0.18 ms, respectively. This result means that the conformation of **A-motif 1** is very similar to that of **A-motif 2** at neutral pH. However, diffusion times (τ_{diff}) of **A-motif 1** and **2** at pH 3.8 are 0.63 ± 0.05 and 0.86 ± 0.07 ms, respectively, which are 3−4 times faster than those determined at pH 7.0. Because the molecular diffusion time is propotional to the hydrodynamic radius of a molecule, the faster diffusion times indicate that the hydrodynamic radii of the conformations of **A-motif 1** and **2** observed at pH 3.8 are 3−4 times smaller than that of the single-stranded structure at neutral pH. This result supports that S-form of **A-motif 1** and **2** at acidic pH and low concentration may have the single-stranded structure with short intramolecular double-stranded regions formed by intramolecular A:A base pairing rather than the extended single-stranded structure. In addition, concerning the directions of phosphate backbone of **A-motif 1** and **2**, they may have different hypothetic single-stranded structures as depicted in Figure 5.

4. CONCLUSIONS

In this study, we designed two different adenine oligomers labeled with FRET donor and acceptor dye (Scheme 1b) and comprehensively investigated the duplex formation by pH and coralyne binding at the single molecule level and in the bulk phase. Results presented here show that **A-motif 1** forms the wire-type duplex at acidic pH, whereas **A-motif 2** becomes the wire-type duplex by the binding of coralyne at neutral pH, supporting that poly(dA) at acidic pH forms a right-handed helical duplex with parallel-mannered chains, whereas the intercalation of coralyne into poly(dA) induces a stable antiparallel duplex. Furthermore, we found that the antiparallel duplex formed by coralyne binding has a rather extended and less twisted structure as compared to parallel duplex formed at acidic pH. On the other hand, upon decreasing the concentration of poly(dA), the parallel duplex formed at acidic pH is converted to S-form, which has the single-stranded structure with short intramolecular double-stranded regions formed by A:A base pairing, while the A-motif−coralyne assembly begins to be dissociated into the single-stranded structure (Figure 5). Although the existence of intramolecular double-stranded regions in poly(A) sequence has been proposed,[20,40] there has been no report that experimentally proved the presence of such structures. Here, we successfully evidenced the existence of intramolecular double-stranded regions in A-motif using various spectroscopic methods, including FCS and single-molecule FRET technique. The result presented here suggests that there is a possibility of the existence of intramolecular duplex region in poly(A) tail in vivo, and this duplex region may affect the biological function of poly(A) tail as suggested by Zarudnaya et al.[20] In addition, this finding is extremely valuable for the nanotechnology that exploits poly(A) or poly(dA) as building blocks because the formation of S-form suggested in this study may affect an overall structure and working efficiency in nanomachine or DNA architecture.

■ ASSOCIATED CONTENT

Supporting Information. Experimental details and additional results. This material is available free of charge via the Internet at http://pubs.acs.org.

■ AUTHOR INFORMATION

Corresponding Author

*Phone: +81-6-6879-8495. Fax: +81-6-6879-8499. E-mail: jkchoi@sanken.osaka-u.ac.jp (J.C.), majima@sanken.osaka-u.ac.jp (T.M.).

■ ACKNOWLEDGMENT

This work has been partly supported by a Grant-in-Aid for Scientific Research (Projects 22245022 and others) from the Ministry of Education, Culture, Sports, Science, and Technology

(MEXT) of the Japanese Government. T.M. thanks the WCU (World Class University) program funded by the Ministry of Education, Science, and Technology through the National Research Foundation of Korea (R31-2008-10035-0) for the support.

REFERENCES

(1) Bacolla, A.; Wells, R. D. *Mol. Carcinog.* **2009**, *48*, 273–285.
(2) Wang, G.; Vasquez, K. M. *Mutat. Res.* **2006**, *598*, 103–119.
(3) Choi, J.; Majima, T. *Chem. Soc. Rev.* **2011**, *40*, 5893−5909.
(4) Wang, C.; Huang, Z.; Lin, Y.; Ren, J.; Qu, X. *Adv. Mater.* **2010**, *22*, 2792–2798.
(5) Modi, S.; M, G. S.; Goswami, D.; Gupta, G. D.; Mayor, S.; Krishnan, Y. *Nat. Nanotechnol.* **2009**, *4*, 325–330.
(6) Saha, S.; Bhatia, D.; Krishnan, Y. *Small* **2010**, *6*, 1288–1292.
(7) Bhatia, D.; Sharma, S.; Krishnan, Y. *Curr. Opin. Biotechnol.* **2011**, *22*, 475–484.
(8) Fahlman, R. P.; Hsing, M.; Sporer-Tuhten, C. S.; Sen, D. *Nano Lett.* **2003**, *3*, 1073–1078.
(9) Chakraborty, S.; Sharma, S.; Maiti, P. K.; Krishnan, Y. *Nucleic Acids Res.* **2009**, *37*, 2810–2817.
(10) Rich, A.; Davies, D. R.; Crick, F. H.; Watson, J. D. *J. Mol. Biol.* **1961**, *3*, 71–86.
(11) Persil, O.; Santai, C. T.; Jain, S. S.; Hud, N. V. *J. Am. Chem. Soc.* **2004**, *126*, 8644–8645.
(12) Chowdhury, S. R.; Islam, M. M.; Kumar, G. S. *Mol. BioSyst.* **2010**, *6*, 1265–1276.
(13) Song, G.; Ren, J. *Chem. Commun.* **2010**, *46*, 7283–7294.
(14) Giri, P.; Suresh Kumar, G. *Mol. BioSyst.* **2010**, *6*, 81–88.
(15) Xi, H.; Gray, D.; Kumar, S.; Arya, D. P. *FEBS Lett.* **2009**, *583*, 2269–2275.
(16) Alberts, B. *Molecular Biology of the Cell*, 5th ed.; Garland Science: New York, 2008.
(17) Janik, B.; Sommer, R. G.; Bobst, A. M. *Biochim. Biophys. Acta* **1972**, *281*, 152–168.
(18) Petrovic, A. G.; Polavarapu, P. L. *J. Phys. Chem. B* **2005**, *109*, 23698–23705.
(19) Finch, J. T.; Klug, A. *J. Mol. Biol.* **1969**, *46*, 597–598.
(20) Zarudnaya, M. I.; Hovorun, D. M. *IUBMB Life* **1999**, *48*, 581–584.
(21) Maggini, R.; Secco; Venturini, M.; Diebler, H. *J. Chem. Soc., Faraday Trans.* **1994**, *90*, 2359–2363.
(22) Xing, F.; Song, G.; Ren, J.; Chaires, J. B.; Qu, X. *FEBS Lett.* **2005**, *579*, 5035–5039.
(23) Gough, A. N.; Jones, R. L.; Wilson, W. D. *J. Med. Chem.* **1979**, *22*, 1551–1554.
(24) Maiti, M.; Kumar, G. S. *J. Nucleic Acids* **2010**, DOI: 10.4061/2010/593408.
(25) Bhadra, K.; Kumar, G. S. *Biochim. Biophys. Acta* **2011**, *1810*, 485–496.
(26) Lv, Z.; Wei, H.; Li, B.; Wang, E. *Analyst* **2009**, *134*, 1647–1651.
(27) Xu, X.; Wang, J.; Yang, F.; Jiao, K.; Yang, X. *Small* **2009**, *5*, 2669–2672.
(28) Zhao, C.; Peng, Y.; Song, Y.; Ren, J.; Qu, X. *Small* **2008**, *4*, 656–661.
(29) Mansoor, S. E.; DeWitt, M. A.; Farrens, D. L. *Biochemistry* **2010**, *49*, 9722–9731.
(30) Choi, J.; Kim, S.; Tachikawa, T.; Fujitsuka, M.; Majima, T. *J. Am. Chem. Soc.* **2011**, *133*, 16146–16153.
(31) Tumpane, J.; Kumar, R.; Lundberg, E. P.; Sandin, P.; Gale, N.; Nandhakumar, I. S.; Albinsson, B.; Lincoln, P.; Wilhelmsson, L. M.; Brown, T.; Norden, B. *Nano Lett.* **2007**, *7*, 3832–3839.
(32) Rasnik, I.; McKinney, S. A.; Ha, T. *Nat. Methods* **2006**, *3*, 891–893.
(33) Cetinkol, O. P.; Hud, N. V. *Nucleic Acids Res.* **2009**, *37*, 611–621.
(34) Joung, I. S.; Persil Cetinkol, O.; Hud, N. V.; Cheatham, T. E., III. *Nucleic Acids Res.* **2009**, *37*, 7715–7727.
(35) Roy, R.; Hohng, S.; Ha, T. *Nat. Methods* **2008**, *5*, 507–516.
(36) Liu, R.; Hu, D.; Tan, X.; Lu, H. P. *J. Am. Chem. Soc.* **2006**, *128*, 10034–10042.
(37) Tan, X.; Nalbant, P.; Toutchkine, A.; Hu, D. H.; Vorpagel, E. R.; Hahn, K. M.; Lu, H. P. *J. Phys. Chem. B* **2004**, *108*, 737–744.
(38) Choi, J.; Kim, S.; Tachikawa, T.; Fujitsuka, M.; Majima, T. *Phys. Chem. Chem. Phys.* **2011**, *13*, 5651–5658.
(39) Neuweiler, H.; Johnson, C. M.; Fersht, A. R. *Proc. Natl. Acad. Sci. U.S.A.* **2009**, *106*, 18569–18574.
(40) Smith, B. L.; Gallie, D. R.; Le, H.; Hansma, P. K. *J. Struct. Biol.* **1997**, *119*, 109–117.